

12-1981

## Contours of constant principal angle and constant principal azimuth in the complex $\epsilon$ plane

R. M.A. Azzam

*University of New Orleans, razzam@uno.edu*

Follow this and additional works at: [https://scholarworks.uno.edu/ee\\_facpubs](https://scholarworks.uno.edu/ee_facpubs)



Part of the [Electrical and Electronics Commons](#), and the [Physics Commons](#)

---

### Recommended Citation

R. M. A. Azzam, "Contours of constant principal angle and constant principal azimuth in the complex  $\epsilon$  plane," *J. Opt. Soc. Am.* 71, 1523-1528 (1981)

This Article is brought to you for free and open access by the Department of Electrical Engineering at ScholarWorks@UNO. It has been accepted for inclusion in Electrical Engineering Faculty Publications by an authorized administrator of ScholarWorks@UNO. For more information, please contact [scholarworks@uno.edu](mailto:scholarworks@uno.edu).

# Contours of constant principal angle and constant principal azimuth in the complex $\epsilon$ plane

R. M. A. Azzam

Department of Electrical Engineering, College of Engineering, University of New Orleans, Lakefront,  
New Orleans, Louisiana 70122

Received May 19, 1981

For light reflection at a planar interface between two homogeneous isotropic media with complex relative dielectric function  $\epsilon$ , we show that the constant-principal-angle contours are a family of semicircles, whereas the constant-principal-azimuth contours are a family of (segments of) hyperbolas in the complex  $\epsilon$  plane. We also find the exact envelope curve of both families and hence determine the domain of the  $\epsilon$  plane of multiple (three) principal angles that is bounded by the envelope curve and the real axis. A unique and peculiar interface with  $\epsilon = (5 - j\sqrt{2})/27$  is shown to have three coincident principal angles of  $30^\circ$  and an associated curve of relative phase shift ( $\Delta$ ) versus angle of incidence that exhibits a distinct shoulder at the principal angle.

## 1. INTRODUCTION

Consider the oblique reflection of a plane wave of light at the planar interface between two homogeneous and isotropic media. The medium of incidence is assumed to be transparent, whereas that of refraction may be absorbing. The reflective (and refractive) properties of the interface are completely determined by the complex relative dielectric function  $\epsilon$ , which is the ratio of the dielectric function of the medium of refraction to that of the medium of incidence. If the incident light is linearly polarized with its electric vibration at an azimuth  $\theta$  from the plane of incidence, the angle of incidence  $\phi$  can be adjusted until the elliptical vibration of the reflected light is aligned with its major and minor axes parallel and perpendicular to the plane of incidence, as in Fig. 1. The angle of incidence under this condition is called the principal angle<sup>1</sup> and is denoted by  $\bar{\phi}$ . The associated principal azimuth,  $\bar{\psi}$ , is the value of  $\theta$  that makes the reflected light circularly polarized. Thus the principal angle and principal azimuth specify angular conditions at which incident linearly polarized light is reflected circularly polarized.

We assume the  $e^{j\omega t}$  time dependence and  $p$  and  $s$  directions parallel and perpendicular to the plane of incidence as in the Nebraska (Muller) conventions.<sup>2</sup> The ratio of  $p$  and  $s$  complex amplitude reflection coefficients,

$$\begin{aligned}\rho &= r_{pp}/r_{ss} \\ &= \tan \psi e^{j\Delta},\end{aligned}\quad (1)$$

becomes

$$\begin{aligned}\bar{\rho} &= \tan \bar{\psi} e^{j\pi/2} \\ &= j \tan \bar{\psi}\end{aligned}\quad (2)$$

at the principal angle, which is also the angle of incidence at which the differential reflection phase shift  $\Delta$  is  $90^\circ$ .

It is generally thought that there is only one principal angle for any given  $\epsilon$ , i.e., for any given interface. However, Holl<sup>3</sup> has shown that there exists a certain domain in the complex plane of the relative refractive index  $N = \epsilon^{1/2}$  where two or three distinct principal angles may correspond to one and the

same  $N$ . Holl specified such a domain approximately and found that the contours of constant principal angle constitute a family of Cassinian curves of different shapes, with the contour for  $\bar{\phi} = 45^\circ$  being the lemniscate of Bernoulli.<sup>3</sup>

By working in the complex  $\epsilon$  plane, instead of that of  $N = \epsilon^{1/2}$ , we show that the contours of constant principal angle ( $\bar{\phi} = \text{constant}$ ) and those of constant principal azimuth ( $\bar{\psi} = \text{constant}$ ) are families of semicircles and hyperbolas, respectively. We also examine thoroughly the conditions of multiple principal angles and determine exactly the domain of the  $\epsilon$  plane of multiple ( $\bar{\phi}, \bar{\psi}$ ) per  $\epsilon$ .

## 2. BASIC RELATIONS

At any angle of incidence  $\phi$ ,  $\epsilon$  is given by<sup>4</sup>

$$\epsilon = \sin^2 \phi + \eta^2 \sin^2 \phi \tan^2 \phi, \quad (3)$$

where

$$\eta = (1 - \rho)/(1 + \rho). \quad (4)$$

$\eta$ , which appears in Eq. (3) and is defined by Eq. (4), can be recognized as a ratio of two unusual reflection coefficients. If  $x$  and  $y$  are transverse directions in the incident and reflected beams that bisect the  $p$  and  $s$  axes (i.e., at  $45^\circ$  and  $135^\circ$  azimuth, respectively, from the plane of incidence), then

$$\eta = r_{xy}/r_{xx}, \quad (5)$$

where  $r_{xx}$  and  $r_{xy}$  are the diagonal ( $x \rightarrow x$ ) and off-diagonal ( $x \rightarrow y$ ) complex reflection coefficients of the interface for incident  $x$ -polarized light.  $\eta$  is also a complex number that represents the reflected polarization state, referred to the  $xy$  coordinate system, when the incident light is linearly  $x$  polarized.

At a principal angle  $\bar{\phi}$ ,  $\rho = j \tan \bar{\psi}$ , and Eq. (4) gives

$$\eta = e^{-j2\bar{\psi}}. \quad (6)$$

If we substitute Eq. (6) into Eq. (3), with  $\phi = \bar{\phi}$ , we get

$$\epsilon = \sin^2 \bar{\phi} + \sin^2 \bar{\phi} \tan^2 \bar{\phi} e^{-j4\bar{\psi}}. \quad (7)$$

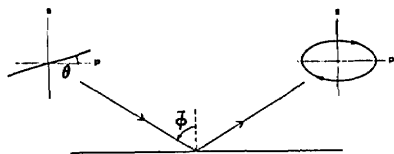


Fig. 1. The principal angle  $\bar{\phi}$  is the angle of incidence at which incident linearly polarized light of any azimuth  $\theta$  is reflected elliptically polarized with major and minor axes aligned parallel ( $p$ ) and perpendicular ( $s$ ) to the plane of incidence. When  $\theta$  equals the principal azimuth  $\bar{\psi}$ , the reflected light is circularly polarized.

### 3. CONTOURS OF CONSTANT PRINCIPAL ANGLE

The  $\bar{\phi} = \text{constant}$  contours in the complex  $\epsilon$  plane can be readily determined by eliminating  $\bar{\psi}$  from Eq. (7); this gives

$$|\epsilon - \sin^2 \bar{\phi}| = \sin^2 \bar{\phi} \tan^2 \bar{\phi}. \quad (8)$$

For a given  $\bar{\phi}$ , Eq. (8) describes a circle with center on the real axis at  $\epsilon = \sin^2 \bar{\phi}$  and radius of  $\sin^2 \bar{\phi} \tan^2 \bar{\phi}$ . Because we assume the  $e^{j\omega t}$  time dependence and passive media,  $\epsilon$  is limited to the lower half of the  $\epsilon$  plane including the real axis. Hence the  $\bar{\phi} = \text{constant}$  contour is a semicircle, as shown in Fig. 2 for  $\bar{\phi} = 40^\circ$ . According to Eq. (7), the angle between a circle radius  $CP$  and the real axis is  $4\bar{\psi}$ . As  $\bar{\psi}$  increases from 0 to  $\pi/4$ ,  $P$  moves along the entire semicircle from  $A$  to  $B$ .

By allowing  $\bar{\phi}$  to change as a parameter, one generates a family of semicircles. Figures 3(a)–3(c) show these  $\bar{\phi} = \text{constant}$  contours for the following ranges of  $\bar{\phi}$ : (a)  $0 \leq \bar{\phi} \leq \bar{\phi}_M$ , (b)  $\bar{\phi}_M \leq \bar{\phi} \leq 45^\circ$ , and (c)  $45^\circ \leq \bar{\phi} < 90^\circ$ , where  $\bar{\phi}_M = \arccos 2^{-1/4} = 32.765^\circ$  is an angle whose significance will be explained shortly. Notice that there are intersections among  $\bar{\phi} = \text{constant}$  semicircles in Fig. 3(a) for  $0 \leq \bar{\phi} \leq 32.765^\circ$ ; semicircles in Fig. 3(b) for  $32.765^\circ \leq \bar{\phi} \leq 45^\circ$  are nonintersecting but intersect those of Fig. 3(a); and semicircles in Fig. 3(c) for  $45^\circ \leq \bar{\phi} < 90^\circ$  are nonintersecting neither among themselves nor with those of Figs. 3(a) and 3(b). At a point of intersection of  $\bar{\phi} = \text{constant}$  contours, more than one principal angle corresponds to the same  $\epsilon$ . This multiplicity of  $\bar{\phi}$  for a given  $\epsilon$  is considered in detail in Section 5. In Fig. 3(c), as  $\bar{\phi}$  approaches  $90^\circ$ , the  $\bar{\phi} = \text{constant}$  contours approach concentric circles with center at  $\epsilon = 1$ .

### 4. CONTOURS OF CONSTANT PRINCIPAL AZIMUTH

If we substitute

$$\epsilon = \epsilon_r + j\epsilon_i \quad (9)$$

into Eq. (7) and break it into its real and imaginary parts, we get

$$\epsilon_r = \sin^2 \bar{\phi} + \sin^2 \bar{\phi} \tan^2 \bar{\phi} \cos 4\bar{\psi}, \quad (10a)$$

$$\epsilon_i = -\sin^2 \bar{\phi} \tan^2 \bar{\phi} \sin 4\bar{\psi}. \quad (10b)$$

To obtain the equation of the  $\bar{\psi} = \text{constant}$  contour, we have to eliminate  $\bar{\phi}$  between Eqs. (10a) and (10b). We find it easier to eliminate  $\bar{\phi}$  between Eq. (10b) and the following equation:

$$\epsilon_i/(\epsilon_r - \sin^2 \bar{\phi}) = -\tan 4\bar{\psi}, \quad (10c)$$

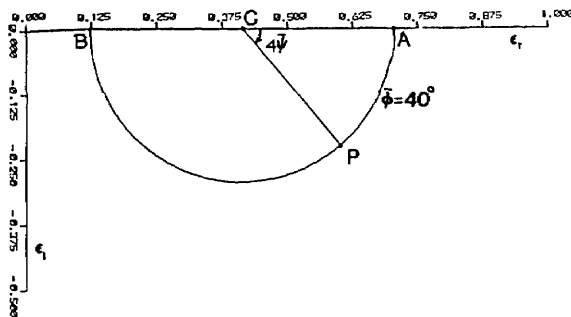
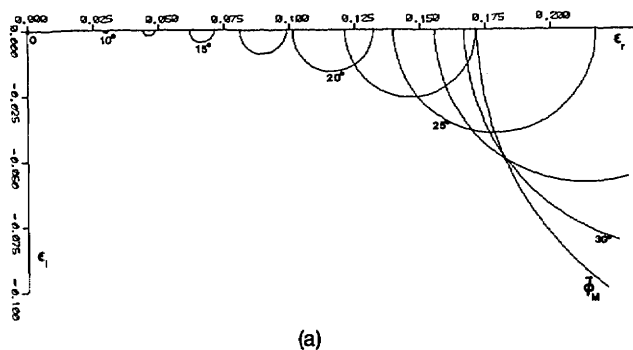
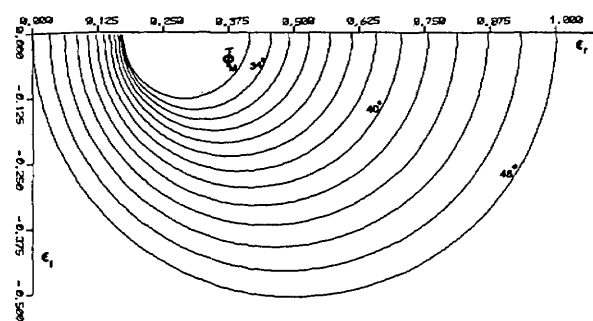


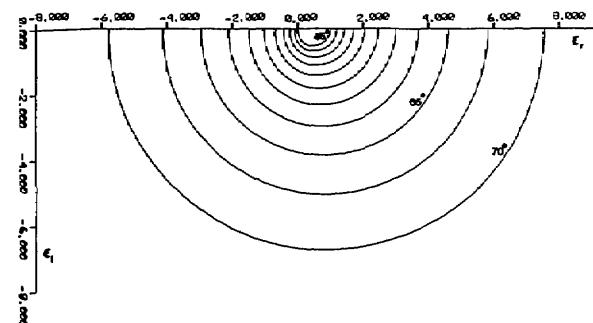
Fig. 2. A constant-principal-angle contour ( $\bar{\phi} = 40^\circ$ ) in the complex  $\epsilon$  plane is a semicircle with center  $C$  on the real axis at  $\sin^2 \bar{\phi}$  and radius  $CP = \sin^2 \bar{\phi} \tan^2 \bar{\phi}$ . The angle between  $CP$  and the real axis equals  $4\bar{\psi}$ , where  $\bar{\psi}$  is the principal azimuth.



(a)



(b)



(c)

Fig. 3. (a) A family of constant-principal-angle semicircles for  $\bar{\phi}$  in the range  $0 \leq \bar{\phi} \leq \bar{\phi}_M$ , where  $\bar{\phi}_M = \arccos 2^{-1/4} = 32.765^\circ$ . The semicircle radius ( $\sin^2 \bar{\phi} \tan^2 \bar{\phi}$ ) increases monotonically with  $\bar{\phi}$ , with increment of  $\bar{\phi}$  between any two successive semicircles of  $2.5^\circ$  (for  $10^\circ \leq \bar{\phi} \leq 30^\circ$ ). (b) Same as in Fig. 3(a) for  $\bar{\phi}_M \leq \bar{\phi} \leq 45^\circ$ .  $\bar{\phi}$  increases from 34 to  $45^\circ$  in steps of  $1^\circ$ . (c) Same as in Fig. 3(a) for  $45^\circ \leq \bar{\phi} \leq 70^\circ$ , with a  $\Delta\bar{\phi}$  step from one semicircle to the next of  $2.5^\circ$ .

which is readily derived from Eqs. (10a) and (10b). If we substitute  $\tan^2 \bar{\phi} = \sin^2 \bar{\phi} / (1 - \sin^2 \bar{\phi})$  into Eq. (10b), we can transform it to a quadratic equation in  $\sin^2 \bar{\phi}$  whose solution is

$$\sin^2 \bar{\phi} = \frac{1}{2} \epsilon_i \csc 4\bar{\psi} \pm \frac{1}{2} (\epsilon_i^2 \csc^2 4\bar{\psi} - 4\epsilon_i \csc 4\bar{\psi})^{1/2}. \quad (11a)$$

From Eq. (10c) we have

$$\sin^2 \bar{\phi} = \epsilon_r + \epsilon_i \cot 4\bar{\psi}. \quad (11b)$$

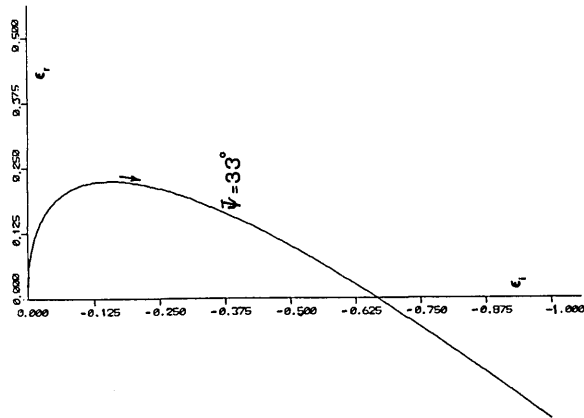


Fig. 4. A constant-principal-azimuth contour ( $\bar{\psi} = 33^\circ$ ) in the complex  $\epsilon$  plane is a segment of a hyperbola that passes through the origin.  $\bar{\phi}$  increases monotonically along the contour in the direction of the arrow from  $0^\circ$  at the origin to  $90^\circ$  at infinity.

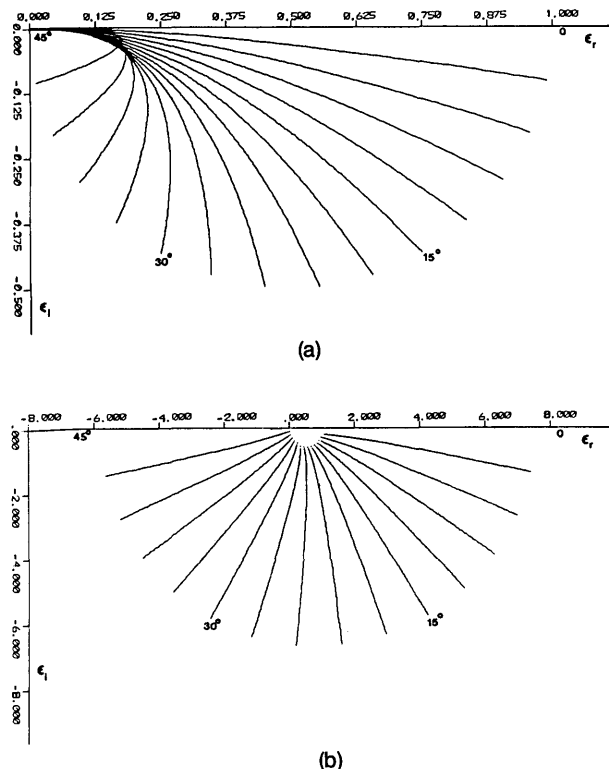


Fig. 5 (a) A family of constant-principal-azimuth contours (hyperbolas) for  $0 \leq \bar{\psi} \leq 45^\circ$  with equal steps of  $3^\circ$ . Along each contour,  $\bar{\phi}$  increases from 0 to  $45^\circ$ . (b) Continuation of the same constant-principal-azimuth contours of Fig. 5(a) obtained by allowing  $\bar{\phi}$  to increase from  $45$  to  $70^\circ$ .

$\bar{\phi}$  is eliminated by equating Eqs. (11a) and (11b); this gives

$$\epsilon_r^2 \sin^2 4\bar{\psi} + \epsilon_i^2 \cos 4\bar{\psi} (\cos 4\bar{\psi} - 1) + \epsilon_r \epsilon_i \sin 4\bar{\psi} (2 \cos 4\bar{\psi} - 1) + \epsilon_i \sin 4\bar{\psi} = 0. \quad (12)$$

Equation (12) is of the second degree of the form

$$Ax^2 + Bxy + Cy^2 + Lx + My + N = 0, \quad (13)$$

where  $L = N = 0$ . The indicator<sup>5</sup> ( $B^2 - 4AC$ ) of Eq. (12) is equal to  $+1$ , so that the equation is of the hyperbolic type, for all values of  $\bar{\psi}$ . The discriminant<sup>5</sup> ( $4ACN - B^2N - AM^2 - CL^2 + BLM$ ) of Eq. (12) is equal to  $-4 \sin^3 4\bar{\psi}$  and is nonzero for  $0 < \bar{\psi} < \pi/4$ . Consequently, Eq. (12) represents a family of hyperbolas in the complex plane of  $\epsilon = (\epsilon_r, \epsilon_i)$ , all passing through the origin because  $N = 0$ . Because we adopt the  $e^{j\omega t}$  time dependence, only portions of these hyperbolas in the lower half-plane  $\epsilon_i \leq 0$  are considered. When  $\bar{\psi} = 0$  or  $\bar{\psi} = \pi/4$ , the discriminant is zero and the corresponding hyperbolas degenerate into straight-line segments coincident with the real axis.

Figure 4 shows the hyperbola of  $\bar{\psi} = 33^\circ$ . It begins at the origin ( $\bar{\phi} = 0$ ) and ends at infinity ( $\bar{\phi} = 90^\circ$ ) and is traced as  $\bar{\phi}$  increases in the direction of the arrow. Figure 5(a) shows a family of  $\bar{\psi} = \text{constant}$  contours (hyperbolas) for values of  $\bar{\psi}$  from 0 to  $45^\circ$  in steps of  $3^\circ$ .  $\bar{\phi}$  increases along each contour from 0 (origin) to  $45^\circ$ . These contours are continued in Fig. 5(b) by letting  $\bar{\phi}$  increase further from  $45$  to  $70^\circ$ . As  $\bar{\phi}$  approaches  $90^\circ$ , the  $\bar{\psi} = \text{constant}$  contours approach a family of straight lines meeting at one point ( $\epsilon = 1$ ) and orthogonal to the nearly concentric semicircles of  $\bar{\phi} = \text{constant}$  of Fig. 3(c).

### 5. MULTIPLE PRINCIPAL ANGLES FOR A GIVEN $\epsilon$

We find it convenient to change variables as follows:

$$\sin^2 \bar{\phi} = u, \quad -4\bar{\psi} = v. \quad (14)$$

In terms of  $u$ , Eq. (8) becomes

$$(\epsilon_r - u)^2 + \epsilon_i^2 = u^4 / (1 - u)^2, \quad (15)$$

which is the Cartesian equation of the family of semicircles of constant principle angle, with  $u$  as a parameter. Equation (15) can be cast as a cubic equation<sup>6</sup> in  $u$ :

$$a_3 u^3 + a_2 u^2 + a_1 u + a_0 = 0, \quad (16)$$

where

$$\begin{aligned} a_0 &= \epsilon_r^2 + \epsilon_i^2, \\ a_1 &= -2(\epsilon_r^2 + \epsilon_i^2) - 2\epsilon_r, \\ a_2 &= (\epsilon_r^2 + \epsilon_i^2) + 4\epsilon_r + 1, \\ a_3 &= -2\epsilon_r - 2. \end{aligned} \quad (17)$$

For a given  $\epsilon = (\epsilon_r, \epsilon_i)$ , the coefficients of the cubic equation, Eq. (16), are determined by Eqs. (17), and its three roots  $u_1, u_2, u_3$  can be found exactly and explicitly.<sup>7</sup> Because  $u = \sin^2 \bar{\phi}$ , a solution is acceptable only if

$$0 \leq u_k \leq 1, \quad k = 1, 2, 3. \quad (18)$$

There is always one acceptable solution for  $u$ , and hence for  $\bar{\phi}$ , for every  $\epsilon$  in the lower half of the complex plane. However,

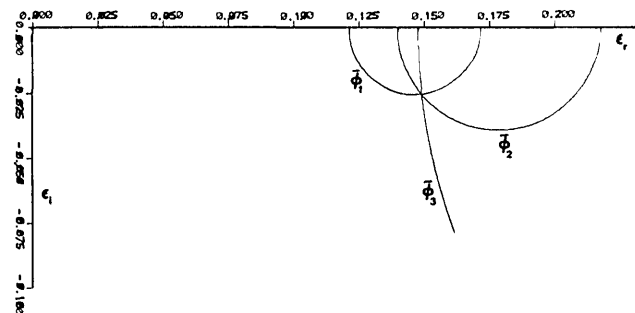


Fig. 6. Three constant-principal-angle semicircles for  $\bar{\phi}_1 = 22.50^\circ$ ,  $\bar{\phi}_2 = 25.00^\circ$ , and  $\bar{\phi}_3 = 38.01^\circ$  intersect at the same point  $\epsilon = 0.15 - j0.025$ .

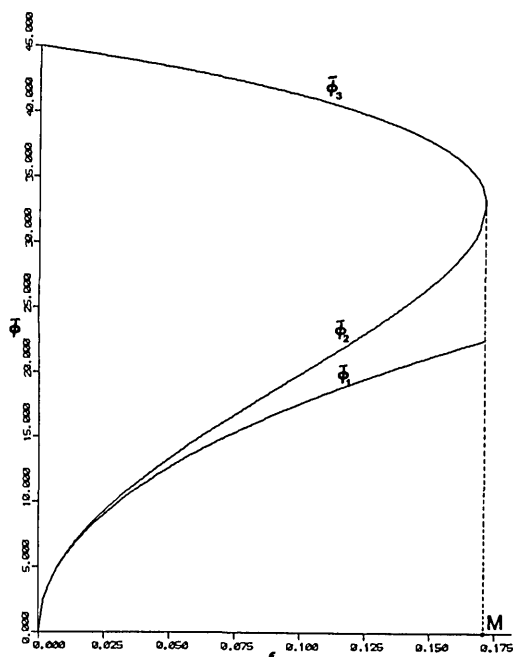


Fig. 7. The three principal angles available when light is internally reflected at interfaces with real  $\epsilon$  in the range  $0 \leq \epsilon \leq 3 - 2\sqrt{2} = 0.1716$  as functions of  $\epsilon$ .  $\bar{\phi}_1$  is the Brewster principal angle, whereas  $\bar{\phi}_2$  and  $\bar{\phi}_3$  are angles of total internal reflection with relative phase shift  $\Delta = 90^\circ$ .  $\bar{\phi}_2$  and  $\bar{\phi}_3$  coincide at M ( $\epsilon = 0.1716$ ).

there exists a small but significant domain of the  $\epsilon$  plane where all three roots of Eq. (16) are acceptable, leading to three principal angles per interface. This domain, whose existence is apparent from Fig. 3(a), can be found by examining the constraint on  $\epsilon$  such that Eq. (16) has three positive real roots between 0 and 1. However, another procedure is used in Section 6 that determines such a domain exactly by its boundaries.

For illustration, let  $\epsilon = 0.15 - j0.025$ , which is expected from Fig. 3(a) to yield multiple principal angles. Substitution of this  $\epsilon$  into Eqs. (17) and solving Eq. (16) gives  $u_1 = 0.1464$ ,  $u_2 = 0.1786$ , and  $u_3 = 0.3792$ . The associated three principal angles are  $\bar{\phi}_1 = 22.50^\circ$ ,  $\bar{\phi}_2 = 25.00^\circ$ , and  $\bar{\phi}_3 = 38.01^\circ$ . Figure 6 shows the corresponding three constant-principal-angle contours intersecting at the same point (0.15, -0.025).

Let us also consider the special case of  $\epsilon$  being real and positive ( $\epsilon = \epsilon_r > 0$ ), which corresponds to interfaces between transparent media. With  $\epsilon_i = 0$ , Eq. (15) reduces to

$$(\epsilon_r - u) = +u^2/(1 - u), \tag{18a}$$

$$(\epsilon_r - u) = -u^2/(1 - u). \tag{18b}$$

Equation (18a) gives one solution,  $u_1$ , for  $u$ :

$$u_1 = \epsilon_r/(\epsilon_r + 1). \tag{19}$$

Equation (18b) can be rewritten as a quadratic equation,

$$2u^2 - (\epsilon_r + 1)u + \epsilon_r = 0, \tag{20}$$

with roots  $u_2, u_3$  given by

$$u_{2,3} = 1/4[(\epsilon_r + 1) \pm (\epsilon_r^2 - 6\epsilon_r + 1)^{1/2}]. \tag{21}$$

Solution  $u_1$ , Eq. (19), is acceptable for all  $\epsilon = \epsilon_r \geq 0$ . However, from Eq. (19), we have  $\epsilon_r = u_1/(1 - u_1) = \tan^2 \bar{\phi}_1$ , so that the principal angle  $\bar{\phi}_1$  is the Brewster angle of the interface. For  $u_2$  and  $u_3$ , Eq. (21), to be real, we must have

$$\epsilon_r^2 - 6\epsilon_r + 1 \geq 0, \tag{22}$$

which is satisfied when<sup>8</sup>

$$0 \leq \epsilon_r \leq 3 - 2\sqrt{2} = 0.1716. \tag{23}$$

Figure 7 plots the three principal angles  $\bar{\phi}_1, \bar{\phi}_2$ , and  $\bar{\phi}_3$  of a transparent interface as functions of  $\epsilon_r$  in the range  $0 \leq \epsilon_r \leq 0.1716$ .  $\bar{\phi}_1$  is the Brewster angle, as we indicated before, whereas  $\bar{\phi}_2, \bar{\phi}_3$  are angles of incidence of total internal reflection with accompanying relative phase shift  $\Delta = 90^\circ$ .

### 6. ENVELOPE CURVE AND REGION OF MULTIPLE PRINCIPAL ANGLES

From Fig. 3(a) it is apparent that the family of semicircles of a constant principal angle has an envelope and that the region of the  $\epsilon$  plane of multiple principal angles is bounded by that envelope and the real axis. To find the equation of the envelope, we first rewrite Eq. (7) with the new variables defined by Eqs. (14):

$$\epsilon = u + [u^2/(1 - u)]e^{jv}. \tag{24}$$

By partial differentiation we find that

$$\left(\frac{\partial \epsilon}{\partial u}\right)_v = \frac{1}{(1 - u)^2} \{[(1 - u)^2 + (2u - u^2)\cos v] + j(2u - u^2)\sin v\}, \tag{25}$$

$$\left(\frac{\partial \epsilon}{\partial v}\right)_u = \frac{u^2}{(1 - u)} (-\sin v + j \cos v). \tag{26}$$

For a point on the envelope,  $(\partial \epsilon / \partial u)_v$  and  $(\partial \epsilon / \partial v)_u$  must be parallel vectors,<sup>9</sup> which, in turn, requires that

$$\frac{-\sin v}{\cos v} = \frac{(1 - u)^2 + (2u - u^2)\cos v}{(2u - u^2)\sin v}. \tag{27}$$

Equation (27) can be simplified to

$$\cos v = [(1 - u)^2 - 1]/(1 - u)^2. \tag{28}$$

Substitution of  $u$  and  $v$  from Eqs. (14) changes Eq. (28) to the following interesting relation between  $\bar{\phi}$  and  $\bar{\psi}$  on the envelope:

$$\cos 4\bar{\psi} = 1 - \sec^4 \bar{\phi}. \tag{29}$$

The maximum value of  $\bar{\phi}$  on the envelope,  $\bar{\phi}_{me}$ , corresponds to  $\sec^4 \bar{\phi} = 2$ , or

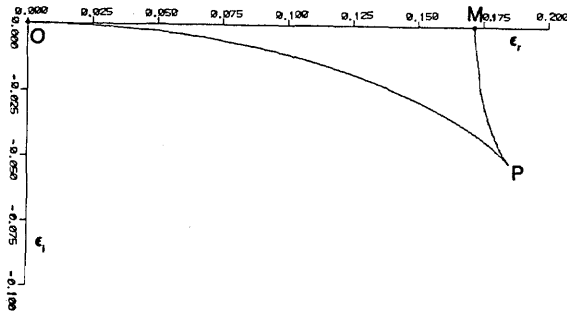


Fig. 8. The common envelope curve *OPM* of the families of contours of constant principal angle and constant principal azimuth. The envelope is described by Eqs. (32) and (33) and represents the locus of all interfaces with two coincident principal angles. At the unique cusplike point *P* all three principal angles collapse and equal  $30^\circ$  [ $\epsilon_P = (5 - j\sqrt{2})/27$ ].

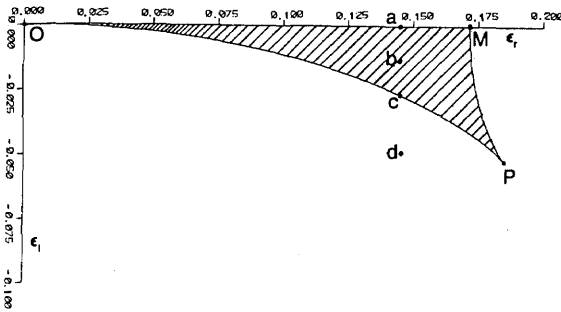


Fig. 9. The domain (shown hatched) of multiple (three) principal angles is bounded by the envelope curve and the real axis. Points *a*, *b*, *c*, and *d* are referred to in Fig. 11.

$$\bar{\phi}_{me} = \arccos(2^{-1/4}) = 32.765^\circ. \quad (30)$$

The associated value of  $\bar{\psi}$  equals  $45^\circ$ . At  $\bar{\phi}_{me}$ ,  $u$  reaches its maximum value given by

$$u_{\max} = 1 - \frac{1}{\sqrt{2}} = 0.293, \quad (31)$$

The corresponding value of  $v$  equals  $-\pi$ . If we put  $(u, v) = (1 - 1/\sqrt{2}, \pi)$  into Eq. (24), we get  $\epsilon = 3 - 2\sqrt{2} = 0.1716$ . Therefore the point of  $\bar{\phi}_{me}$  lies on the real axis and corresponds to the maximum real  $\epsilon$  for multiple principal angles, Eq. (23). (This is point *M*, Fig. 7, where the two principal angles of total internal reflection coincide.)

We return to the equation of the envelope and now find it by substituting Eq. (28) into Eq. (24); this gives  $\epsilon = \epsilon_r + j\epsilon_i$ , where

$$\epsilon_r = u + [u^3(u - 2)/(1 - u)^3], \quad (32a)$$

$$\epsilon_i = (2u^6 - 4u^5 + u^4)^{1/2}/(1 - u)^3, \quad (32b)$$

$$0 \leq u \leq 1 - \frac{1}{\sqrt{2}} = 0.293. \quad (33)$$

Equations (32) are the parametric equations of the envelope curve, with the parameter  $u$  limited to the range of Eq. (33). Figure 8 shows the envelope curve as exactly determined by Eqs. (32) and (33). This same curve is also the envelope of the family of constant-principal-azimuth hyperbolas of Fig. 5(a).

In Fig. 8  $P$  represents an interesting and peculiar cusplike point. At  $P$ ,  $\epsilon_i$  reaches its maximum negative value. By differentiation of Eq. (32b),  $d\epsilon_i/du$  is determined. Setting this derivative equal to zero gives the following equation:

$$u^3(4u^2 - 9u + 2) = 0. \quad (34)$$

The triple root  $u = 0$  indicates that the envelope curve is tangent to the real axis at the origin *O*, as is evident in Fig. 8. The quadratic term in Eq. (34) gives one acceptable root ( $u < 1$ ) that specifies  $u$  at *P*:

$$u_P = \frac{1}{4}. \quad (35)$$

If we substitute  $u = 1/4$  in Eqs. (32), we determine  $\epsilon$  at *P*,

$$\epsilon_P = (5 - j\sqrt{2})/27. \quad (36)$$

Substitution of  $\epsilon_P$ , Eq. (36), into Eqs. (17) shows that the cubic Eq. (16) reduces to

$$\left(u - \frac{1}{4}\right)^3 = 0. \quad (37)$$

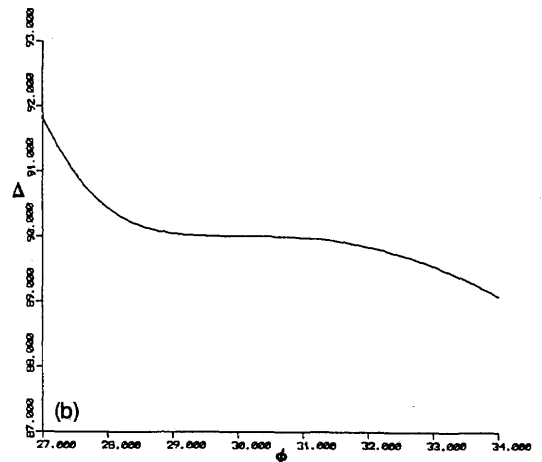
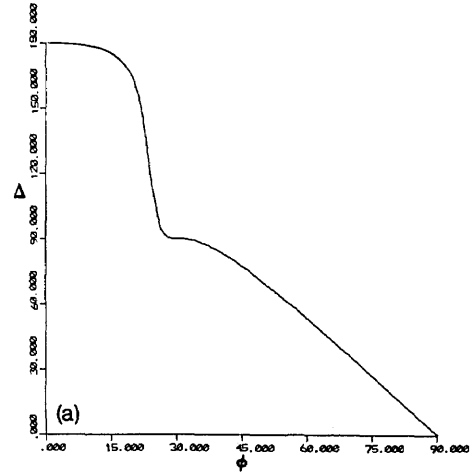


Fig. 10. (a) The relative phase shift  $\Delta$  versus angle of incidence  $\phi$  for the peculiar interface of  $\epsilon_P = (5 - j\sqrt{2})/27$ . Coincidence of all three principal angles produces a pronounced shoulder at  $\Delta = 90^\circ$ ,  $\phi = 30^\circ$ . (b) A magnified view of the shoulder region of Fig. 10(a).

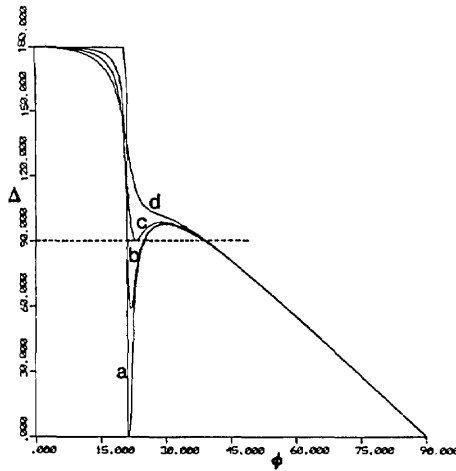


Fig. 11.  $\Delta$ -versus- $\phi$  curves for four values of  $\epsilon$  ( $\epsilon_a = 0.14$ ,  $\epsilon_b = 0.14 - j0.012$ ,  $\epsilon_c = 0.14 - j0.024$ , and  $\epsilon_d = 0.14 - j0.05$ ) that correspond to points on the boundaries a, c, within b, and outside d of the domain of multiple principal angles, as marked on Fig. 9.

Thus  $u = u_P = 1/4$  is a triple root, which indicates that at the point P all three principal angles coincide. This triple principal angle is given by

$$\bar{\phi}_P = \arcsin u_P^{1/2} = \arcsin 1/2 = 30^\circ. \tag{38}$$

The associated principal azimuth is obtained by Eq. (29) as

$$\bar{\psi}_P = 1/4 \arccos(-7/9) = 35.264^\circ. \tag{39}$$

In Fig. 9 the domain of multiple principal angles is the hatched area bounded by the envelope curve  $OPM$  and the segment of the real axis  $OM$ . The multiple principal angles that correspond to points along the real axis between O and M were discussed in Section 5 and are plotted in Fig. 7. The envelope curve  $OPM$  is the locus of  $\epsilon$  such that two of the three possible principal angles coincide, with P being the only point where all three principal angles are identical. As the envelope curve is traced from O to P to M, the double principal angle  $\bar{\phi}_{1,2}$  increases monotonically from 0 to 30 to 32.765°, while the remaining third principal angle  $\bar{\phi}_3$  decreases from 45 to 30 to 22.5°, respectively. The principal azimuth  $\bar{\psi}$  changes along the envelope from 22.5° at O to 35.264° at P to 45° at M, respectively. Every point within the hatched domain represents an interface with three distinct principal angles in the range

$$0 \leq \bar{\phi} \leq 45^\circ. \tag{40}$$

### 7. RELATIVE PHASE SHIFT $\Delta$ AS A FUNCTION OF ANGLE OF INCIDENCE

Figure 10(a) shows the relative phase shift  $\Delta$  as a function of angle of incidence  $\phi$  for the peculiar interface with  $\epsilon_P = (5 -$

$j\sqrt{2})/27$ , which is characterized by three coincident principal angles. The curve has a pronounced shoulder where  $\Delta = 90^\circ$ , in the vicinity of the triple principal angle of 30°. This shoulder appears magnified in Fig. 10(b). We have verified that there is nothing unusual about the behavior of other reflection parameters associated with that same interface.

For completeness, we show in Fig. 11 the behavior of  $\Delta$  as a function of  $\phi$  for four values of  $\epsilon$ , namely, (a)  $\epsilon = 0.14 - j0$ , (b)  $\epsilon = 0.14 - j0.012$ , (c)  $\epsilon = 0.14 - j0.024$ , and (d)  $\epsilon = 0.14 - j0.05$ . The corresponding points are marked in Fig. 9. Points a and c are on the boundaries of the domain of multiple principal angles; b is inside and d is outside that domain. Intersections of the  $\Delta$ -versus- $\phi$  curve with the line  $\Delta = 90^\circ$  define the principal angles. For case (a), there are three intersections, the first being the Brewster principal angle and the remaining two the principal angles of total internal reflection. Case (b) is typical of the situation of an interface with three distinct principal angles. Case (c) is a limiting case when two of the three principal angles coincide, whereas (d) represents the normal condition of only one principal angle.

### 8. SUMMARY

We have determined the nature of the constant-principal-angle and constant-principal-azimuth contours of an interface as families of semicircles and hyperbolas, respectively, in the complex plane of the relative dielectric function  $\epsilon$ . We have determined exactly the common envelope curve of these families. The domain of multiple (three) principal angles is bounded by such an envelope and the real axis. We have discovered a unique and peculiar interface with  $\epsilon = (5 - j\sqrt{2})/27$  that is characterized by three coincident principal angles ( $\bar{\phi} = 30^\circ$ ) and an associated  $\Delta$  versus  $\phi$  curve with a pronounced shoulder feature.

### REFERENCES

1. M. Born and E. Wolf, *Principles of Optics*, 5th ed. (Pergamon, New York, 1975), p. 618.
2. R. H. Muller, "Definitions and conventions in ellipsometry," *Surf. Sci.* **16**, 14-33 (1969).
3. H. B. Holl, "Specular reflection and characteristics of reflected light," *J. Opt. Soc. Am.* **57**, 683-690 (1967).
4. See, for example, R. M. A. Azzam and N. M. Bashara, *Ellipsometry and Polarized Light* (North-Holland, Amsterdam, 1977), p. 274.
5. See, for example, F. H. Miller, *Analytic Geometry and Calculus* (Wiley, New York, 1949), pp. 222-224.
6. This is significantly simpler than Eq. (11) of Ref. 3, which is of the 8th degree in  $\tan \bar{\phi}$ .
7. See, for example, S. M. Selby, ed., *Standard Mathematical Tables*, 20th ed. (Chemical Rubber Company, Cleveland, Ohio, 1972), pp. 103-105.
8. Condition (22) is also satisfied when  $\epsilon_r \geq 3 + 2\sqrt{2}$ , but this leads to unacceptable solutions for  $u_2$  and  $u_3$ .
9. G. Zwikker, *The Advanced Geometry of Plane Curves and Their Applications* (Dover, New York, 1963), Chap. 13.